Reprinted from

George J. Dvorak (Ed.)

# Inelastic Deformation of Composite Materials

IUTAM Symposium, Troy, New York
May 29-June 1, 1990



Springer-Verlag
New York Berlin Heidelberg London
Paris Tokyo Hong Kong Barcelona

# Compressive Failure of Fibre Composites Due to Microbuckling

N.A. Fleck[†] and B. Budiansky[*]

[†]Cambridge University Engineering Department, Trumpington Street, Cambridge, CB2 1PZ, England.

[*]Division of Applied Sciences, Harvard University, Cambridge, Massachusetts, 02138, U.S.A.

**ABSTRACT**

The dominant compressive failure mechanism of modern fibre composites is microbuckling. This is demonstrated in the form of a fracture map. For polymer matrix composites microbuckling is a plastic event. An analysis is presented of both elastic and plastic microbuckling of unidirectional composites under remote axial and shear loading. The effects of fibre misalignment and inclination of the band are included. We find that a simple rigid-perfectly plastic analysis suffices for plastic microbuckling; it demonstrates that the axial compressive strength increases with decreasing fibre misalignment, increasing shear strength of the matrix, and decreasing remote shear stress. Finally, a calculation is performed of the remote axial and shear stress required to propagate an existing microbuckle. We find that the axial propagation stress is typically less than the shear yield stress of the matrix material.

## 1. INTRODUCTION

Most fibre reinforced polymer matrix composites have a compressive strength less than their tensile strength

due to microbuckling of the load bearing fibres aligned with the loading direction. In many applications compressive strength is a design limiting feature. Over the past ten years significant improvements have been made to the tensile strength, impact resistance and toughness of these composites. Unfortunately, compressive strength has shown little concomitant improvement.

In this paper, previous experimental studies and theoretical models of microbuckling are reviewed. A new analysis of microbuckling is presented, based upon the kink band analysis of Budiansky (1983). The composite is subjected to remote axial compression and shear. Material inside and outside of the kink band is taken to be homogeneous but anisotropic. The kink band response is calculated for a variety of constitutive behaviours: (1) elastic, (2) rigid-perfectly plastic, and (3) elastic-perfectly plastic. An analysis is then given for the remote axial and shear stress required to propagate a microbuckle zone into undamaged material across the section of a specimen. The analysis is based upon a simple energy balance. We find remarkably low values for the propagation stress. This suggests that the compressive failure stress of large sheet structures containing a microbuckle near a stress raiser may be much less than that predicted for small undamaged specimens.

The paper deals only with the response of unidirectional unnotched composites. In many practical applications notched multi-directional composites are used. A design methodology is now emerging to deal

with the effects of notches and off-axis plies (see for example, Starnes and Williams (1982), Rhodes, Mikulas and McGowan (1984), Soutis and Fleck (1990) and Soutis, Fleck and Smith (1990)).

## 2. PREVIOUS THEORETICAL WORK

Rosen (1965) assumed that compressive failure is by elastic microbuckling: he modelled the fibres as columns supported by an elastic foundation. He recognised that the composite plate may be a short stiff structure which does not buckle in compression on the macroscale, but the individual fibres have small diameters and buckle as slender columns on the microscale. Two possible buckling modes were distinguished, the shear mode and the extension mode. For the shear mode, shear deformation occurs in the matrix material, and the compressive strength $\sigma_c$ is given by,

$$\sigma_c = \frac{G_m}{1-v_f} \qquad (2.1)$$

where $G_m$ is the shear modulus of the matrix and $v_f$ is the fibre volume fraction. In the extension mode, matrix material suffers direct straining in a direction transverse to the fibre axis. The shear mode predicts a lower strength than the extension mode and is assumed to dominate.

The Rosen anaysis overpredicts strength typically by a factor of four. This suggests that microbuckling is a plastic rather than an elastic event. Several investigators (eg. Lager and June

(1969)) have introduced empirical correction factors in order to improve the agreement between the Rosen theory and experiment.

Argon (1972) and Budiansky (1983) identified the shear yield stress k of the matrix material and the initial misalignment angle $\bar{\phi}$ of fibres in the microbuckled band as the main factors governing the compressive strength.The misalignment angle $\bar{\phi}$, and band inclination $\beta$ are defined in the insert in Fig.1. For a

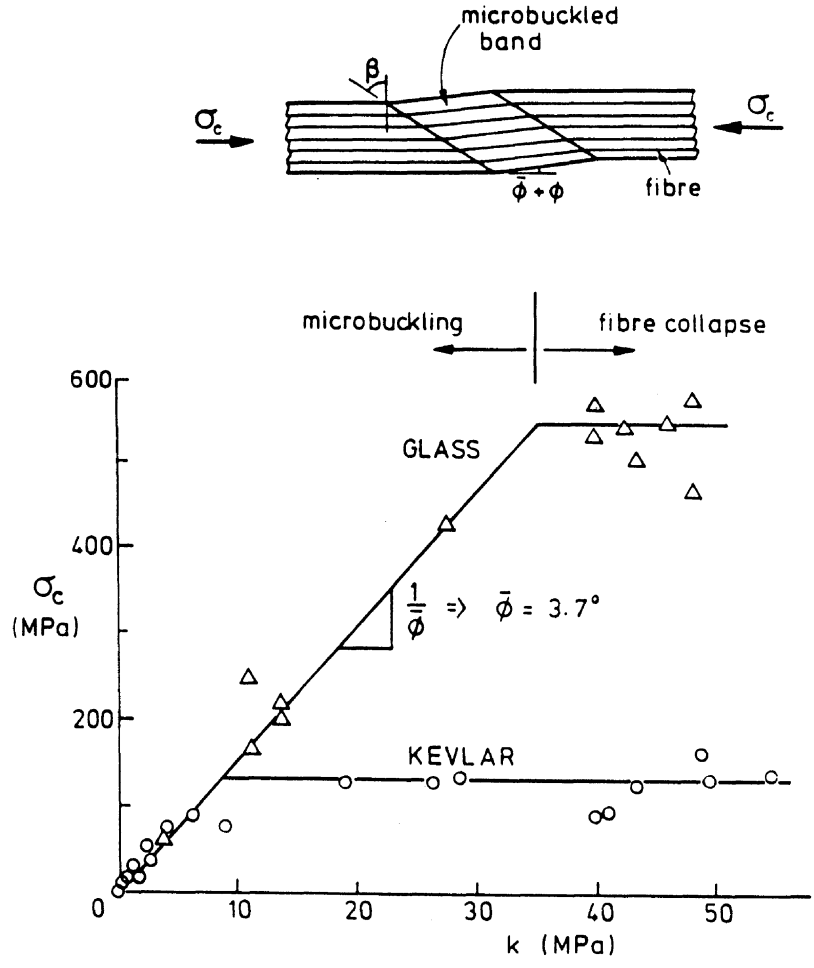


Fig.1: Effect of shear yield stress k of polyester matrix upon compressive strength $\sigma_c$ of glass and Kevlar composites. Data taken from Piggott and Harris (1980).

rigid-perfectly plastic matrix material, Budiansky found that the compressive strength $\sigma_c$ is given by

$$\sigma_c = \frac{k^*}{\phi} \tag{2.2}$$

where,

$$k^* \equiv k \left(1 + \left(\frac{\sigma_{Ty}}{k}\right)^2 \tan^2\beta\right)^{\frac{1}{2}} \tag{2.3}$$

and $\sigma_{Ty}$ is the yield stress of the composite transverse to the fibre direction.

There was little need to include fibre bending explicitly in the analysis: a kinking analysis suffices wherein material in the microbuckled band is treated as a homogeneous anisotropic solid. This approach is developed later in the present paper.

Recently, Steif (1988) has modelled the effect of fibre-matrix debonding upon the elastic microbuckling of fibre composites. The model is an adaptation of the Rosen analysis to situations where slip occurs at the fibre-matrix interface; slip begins when the interfacial shear stress attains a critical value. Interfacial shear failure is similar in many respects to shear yielding of the matrix. Steif's model gives reasonable predictions for ceramic matrix composites when the wavelength of the buckle equals the specimen length. This assumption is unrealistic.

## 3. AVAILABLE EXPERIMENTAL EVIDENCE

From the published literature it is apparent that unidirectional composites fail by two distinct failure mechanisms, fibre microbuckling and fibre collapse.

When the matrix yield stress is sufficiently

high, the fibres suffer compressive collapse. This is due to fibre yielding in the case of steel or Kevlar fibres (see Moncunill de Ferran and Harris (1970), Greszczuk (1972, 1975), Piggott and Harris (1980), and Piggot (1981)). Alternatively, fibre collapse is by compressive fracture from defects in the case of carbon fibres or glass fibres (see Ewins and Ham (1973), Ewins and Potter (1980), and Piggott and Harris (1980)).

Available experimental evidence for polymer matrix composites supports the hypothesis that microbuckling is a plastic rather than an elastic phenomenon. A summary of the measured compressive strengths for unidirectional, carbon fibre polymer matrix composites is given in Table 1. The first three

| Composite System | Ref. | $\sigma_c$ (MPa) | $\frac{G}{1-v_f}$ (MPa) | k (MPa) | $\bar{\phi}$ |
|---|---|---|---|---|---|
| T800/924C | Soutis (1989) | 1615 | 6000 | 60 | 2.6° |
| HITEX 12K/E7jK8 | U.S.Polymeric (1990) | 1447 | 5510 | 40 | 1.4° |
| HITEX 46-3B/E7K8T | U.S.Polymeric (1990) | 1274 | 4400 | 67 | 3.0° |
| AS4/PEEK | Jelf (1990) | 1200 | 4000 | 78 | 3.4° |
| HS/MY720 (Woven) | Curtis and Bishop (1984) | 400 | 3000 | 55 | 7.5° |

Table 1: Comparison of measured compressive strength $\sigma_c$ of unidirectional carbon fibre polymer matrix composites with predictions of the Rosen model, equation 2.1 and the Budiansky model, equation 2.2.

data sets refer to carbon fibre epoxy composites, the system AS4/PEEK is a carbon fibre Peek composite, and the system HS/MY720 refers to a carbon fibre epoxy 0°/90° woven layup. The table includes predicted strengths by the Rosen (1965) model, and the inferred misalignment angle $\bar{\phi}$ by substituting strength values $\sigma_c$ and k into equation 2.2. For simplicity we assume $\beta = 0$ so that $k^* = k$. The error in the inferred values of $\bar{\phi}$ is at most 20% by this approximation, for typical values of $E_T/G$ and $\beta$. We conclude from Table 1 that the Rosen model overpredicts compressive strength by a factor of approximately 4. The inferred values for $\bar{\phi}$ from Budiansky's model, equation 2.2, agree with typical measurements of $\bar{\phi}$, Jelf (1990). For polymer matrix composites, the matrix yields rather than microcracks. We are justified in viewing k as a plastic yield stress.

Direct experimental evidence to support equation 2.2 comes from measurements of the microbuckling strength of glass fibre and Kevlar fibre reinforced polyester by Piggott and Harris (1980). They varied the matrix shear yield stress by controlling the state of polyester resin cure from just jelled to fully cured. The compressive strength is proportional to k, provided that failure is by microbuckling, see Fig.1. This behaviour supports equation 2.2. The slope of the graph in Fig. 1 gives $\bar{\phi} = 3.7°$, assuming $\beta = 0$. When k is increased to sufficiently high values the glass or Kevlar fibres collapse prior to microbuckling.

Early carbon fibre epoxy composites failed by fibre collapse at test temperatures below approximately 100°C, see Fig. 2. At higher temperatures microbuckling occurred; the progressive decrease in microbuckling strength with increasing temperature T for T > 100°C is associated with the decrease in matrix shear yield stress k with increasing T, in accordance with equation 2.2. Over the last decade the compressive strength of carbon fibres has doubled, while epoxy matrices have changed little in strength

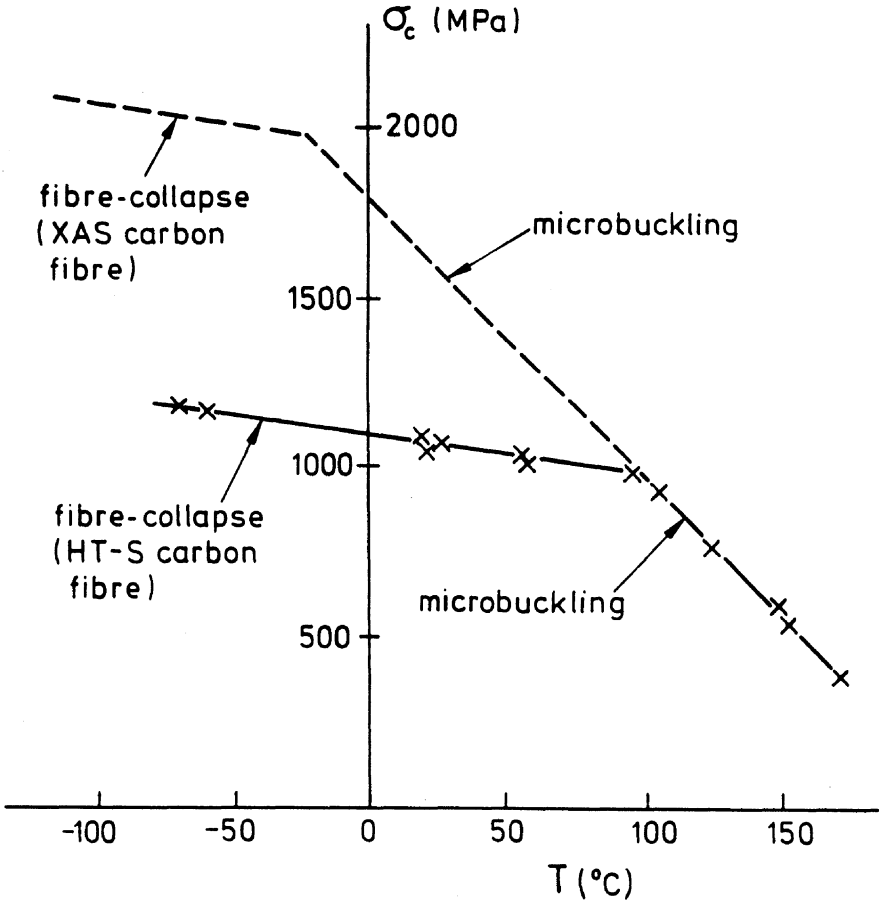


Fig. 2: Effect of temperature T upon failure strength $\sigma_c$ of carbon fibre epoxy matrix composites. Experimental data x-x are taken from Ewins and Potter (1980). The dotted line gives the typical response of more recent systems.

due to demands for high impact strength and high toughness of the composite. Thus the transition temperature from microbuckling to fibre collapse has shifted from approximately 100°C to -40°C (Barker and Balasundaram (1987)), as shown in Fig. 2. Thus present day carbon fibre epoxy composites fail by microbuckling at ambient and at elevated temperatures.

The failure mechanisms exhibited by a unidirectional fibre composite may be summarised in a fracture diagram, with axes $k/\bar{\phi}$ and $G_m/(1-v_f)$, as shown in Fig. 3. Failure is by three distinct mechanisms:

1. Elastic microbuckling. Rosen's analysis predicts a microbuckling strength $\sigma_c$ given by equation 2.1.

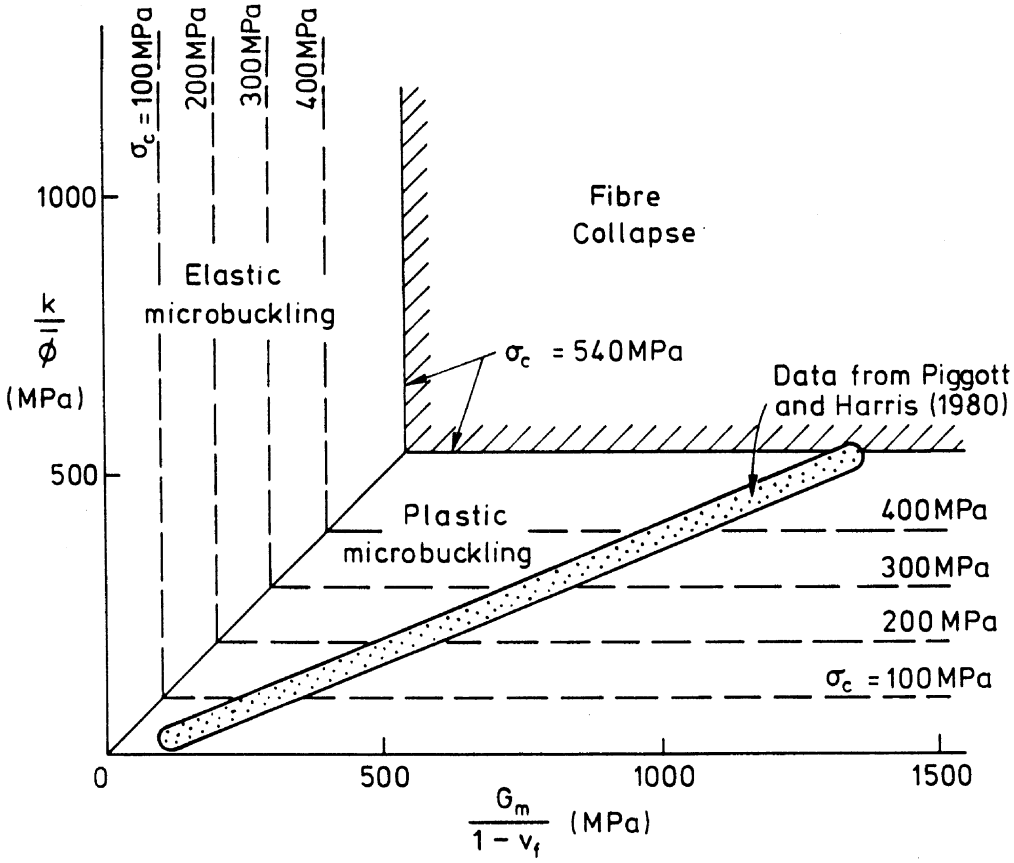


Fig.3: Fracture map for glass fibre polyester matrix composite. Data taken from Piggott and Harris (1980).

2. Plastic microbuckling. The Budiansky analysis predicts a strength given by equation 2.2. For simplicity we assume $\beta = 0$, hence $k^* = k$.

3. Fibre collapse. This occurs when the stress in the fibres attains a critical fracture value $\sigma_f$, such that

$$\sigma_c = v_f \sigma_f \qquad (3.1)$$

The fracture diagram contains contours of compressive strength $\sigma_c$ given by equations 2.1-2.3 and 3.1. The boundary of the fibre collapse regime depends upon fibre volume fraction $v_f$: otherwise the diagram is unique for a given fibre reinforcement.

Data for glass fibre reinforced polyester are included in Fig. 3, taken from the work of Piggott and Harris (1980). The data are replotted from Fig. 1. The experimental values support the common finding that the yield stress and elastic stiffness of polymer matrices scale in a linear fashion: thus the compressive strength of the fibre composite varies linearly with elastic modulus. This has led several investigators (for example Dow and Gruntfest (1960) and Rosen (1965)) to conclude erroneously that microbuckling is an elastic event for polymer matrix composites.

It is clear from the fracture diagram that the maximum attainable compressive strength is dictated by the intrinsic compressive fracture strength of the fibres. This strength is rarely achieved in practice for polymer matrix composites; requirements for high composite toughness and impact strength dictate the use of matrices with a low yield stress and high ductility.

Thus, plastic microbuckling is the usual failure mode in compression.

The ceramic matrix of ceramic fibre/ceramic matrix composites displays a non-linear response due to plasticity or to microcracking, Evans and Adler (1978). A plastic microbuckling analysis remains appropriate for such systems.

Preliminary unpublished tests by the authors show that elastic microbuckling occurs in a glass fibre/silicone rubber matrix composite. No systematic experimental investigations of elastic microbuckling in elastomeric matrix composites were found from the literature.

## 4. KINKING ANALYSIS

We shall analyse the behaviour of a kinked band of infinite length and finite width w, oriented at an angle $\beta$ as shown in Fig. 4. First we consider the

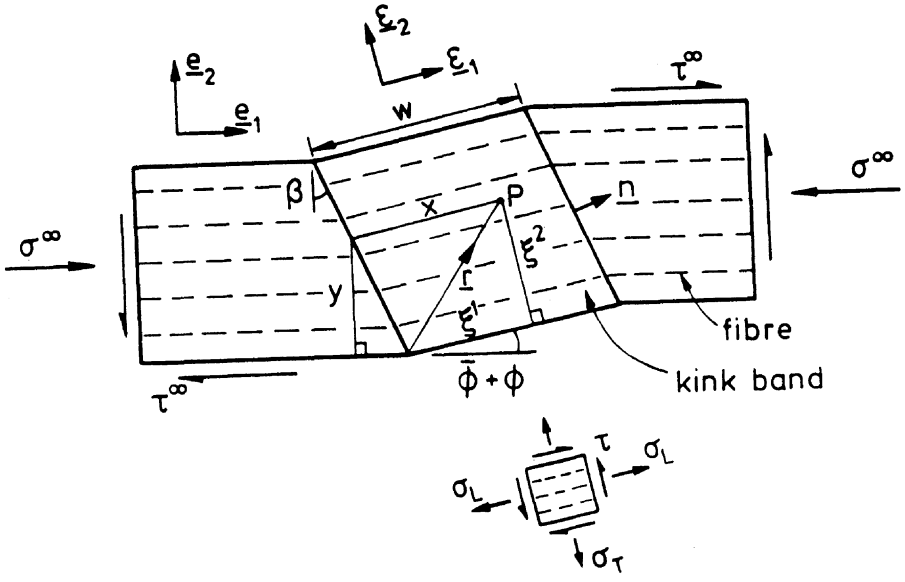


Fig.4: Detailed geometry of kink band.

kinematics and equilibrium of the band. In subsequent sections we explore the effect of the constitutive behaviour upon the buckling response.

### 4.1 Kinematics

We assume inextensional fibres but allow the composite to undergo direct straining transverse to the fibre direction, and shear straining parallel to the fibre direction. The fibres are assumed to have broken along the boundaries of the band. We smear out the fibres and matrix, and consider the composite to behave as a homogeneous anisotropic solid. Fibre bending is not treated explicitly; Budiansky has included the effects of fibre bending elsewhere, Budiansky (1983). He found that except for its role in setting the kink band width, fibre bending has only a small influence on the collapse response and can be neglected for most practical applications.

Consider the buckled band shown in Fig. 4. An arbitrary point P has a position vector $\underline{r}$,

$$\underline{r} = \xi_1 \, \underline{\epsilon}_1 + \xi_2 \, \underline{\epsilon}_2 \tag{4.1}$$

in terms of Cartesian co-ordinates $(\xi_1, \xi_2)$ and fixed orthonormal base vectors $(\underline{\epsilon}_1, \underline{\epsilon}_2)$ which are instantaneously aligned with the fibre direction in the band. The velocity $\underline{v}$ of the point P is

$$\underline{v} = y \, \dot{\gamma}^{\infty} \, \underline{e}_1 + x\dot{\phi} \, \underline{\epsilon}_2 \tag{4.2}$$

where $\dot{\gamma}^{\infty}$ is the remote shear strain rate parallel to the unbuckled fibres, $\dot{\phi}$ is the rotation rate of the fibres in the band, and the fixed unit vector $\underline{e}_1$, and lengths x and y are defined in Fig. 4. We assume the

remote direct strain rate transverse to the fibres equals zero.

The velocity strain rate $\dot{\underset{\sim}{\epsilon}}$ in the band is

$$\dot{\underset{\sim}{\epsilon}} = \tfrac{1}{2} (\underline{\nabla}\, \underline{v} + (\underline{\nabla}\, \underline{v})^T) \qquad (4.3)$$

where the superscript T denotes the transpose and the gradient operator $\underline{\nabla}$ is

$$\underline{\nabla} = \underline{\epsilon}_1 \frac{\partial}{\partial \xi_1} + \underline{\epsilon}_2 \frac{\partial}{\partial \xi_2} \qquad (4.4)$$

The quantitites x, y, $\xi_1$ and $\xi_2$ are related by

$$x = \xi_1 + \xi_2 \tan (\beta - \bar{\phi} - \phi)$$

and, $$y = \xi_2 \cos\beta \sec (\beta - \bar{\phi} - \phi) \qquad (4.5)$$

Here, $\bar{\phi}$ is the initial misalignment angle of fibres in the band; it serves as an imperfection.

Unit vectors $\underline{e}_1$ and $\underline{e}_2$, aligned with respect to the remote fibre direction as shown in Fig. 4, can be resolved into the $\underline{\epsilon}_1$ and $\underline{\epsilon}_2$ directions as,

$$\underline{e}_1 = \underline{\epsilon}_1 \cos(\bar{\phi} + \phi) - \underline{\epsilon}_2 \sin(\bar{\phi} + \phi)$$

$$\underline{e}_2 = \underline{\epsilon}_1 \sin(\bar{\phi} + \phi) + \underline{\epsilon}_2 \cos(\bar{\phi} + \phi) \qquad (4.6)$$

We can now evaluate the strain rate via equations 4.2 - 4.7, to give

$$\dot{\underset{\sim}{\epsilon}} = (\dot{\phi}\tan(\beta-\bar{\phi}-\phi) - \dot{\gamma}^{\infty} \cos\beta \sin(\bar{\phi}+\phi) \sec(\beta-\bar{\phi}-\phi))\underline{\epsilon}_2\underline{\epsilon}_2$$

$$+ \tfrac{1}{2}(\dot{\phi}+\dot{\gamma}^{\infty}\cos\beta\cos(\bar{\phi}+\phi)\sec(\beta-\bar{\phi}-\phi))(\underline{\epsilon}_1\underline{\epsilon}_2 + \underline{\epsilon}_2\underline{\epsilon}_1) \qquad (4.7)$$

But $\dot{\underset{\sim}{\epsilon}}$ equals $[\dot{e}_T\ \underline{\epsilon}_2\underline{\epsilon}_2 + \tfrac{1}{2}\ \dot{\gamma}(\underline{\epsilon}_1\underline{\epsilon}_2 + \underline{\epsilon}_2\underline{\epsilon}_1)]$ where by definition $\dot{e}_T$ is the direct strain rate transverse to the fibres in the band, and $\dot{\gamma}$ is the shear strain rate in the band. Identification of this

expression for $\dot{\underset{\sim}{\epsilon}}$ with equation 4.7 gives,

$$\dot{e}_T = \dot{\phi}\tan(\beta-\bar{\phi}-\phi) - \dot{\gamma}^{\infty} \cos\beta \sin(\bar{\phi}+\phi) \sec(\beta-\bar{\phi}-\phi)$$

and, $$\dot{\gamma} = \dot{\phi} + \dot{\gamma}^{\infty} \cos\beta \cos(\bar{\phi} + \phi) \sec(\beta - \bar{\phi} - \phi) \quad (4.8)$$

For the case of vanishing remote shear, equations 4.8 may be integrated directly to give,

$$e_T = \ell n \left[\frac{\cos(\beta-\bar{\phi}-\phi)}{\cos(\beta-\bar{\phi})}\right]$$

and $$\gamma = \phi. \quad (4.9)$$

The band boundary rotates at a rate $\dot{\beta}$ which depends upon the remote shear strain rate $\dot{\gamma}^{\infty}$,

$$\dot{\beta} = - \dot{\gamma}^{\infty} \cos^2\beta \quad (4.10)$$

Integration of 4.10 yields,

$$\tan\beta = \tan\beta_o - \gamma^{\infty} \quad (4.11)$$

where $\beta_o$ is the initial inclination of the band.

## 4.2 Equilibrium

Now consider equilibrium of the band. Equating the traction on both sides of the band boundary gives,

$$\underline{n} \cdot \underline{\sigma}^{\infty} = \underline{n} \cdot \underline{\sigma} \quad (4.12)$$

where $\underline{n} = \underline{e}_1 \cos\beta + \underline{e}_2 \sin\beta$ is the unit normal to the band, the remote stress $\underset{\sim}{\sigma}^{\infty}$ is,

$$\underset{\sim}{\sigma}^{\infty} = - \sigma^{\infty} \underline{e}_1 \underline{e}_1 + \tau^{\infty} (\underline{e}_1 \underline{e}_2 + \underline{e}_2 \underline{e}_1) \quad (4.13)$$

and the stress inside the band $\underset{\sim}{\sigma}$ is,

$$\underset{\sim}{\sigma} = \sigma_L \underline{e}_1 \underline{e}_1 + \sigma_T \underline{e}_2 \underline{e}_2 + \tau(\underline{e}_1 \underline{e}_2 + \underline{e}_2 \underline{e}_1) \quad (4.14)$$

Here $\sigma_L$ is the direct stress in the fibre direction.

Substitution of 4.13 and 4.14 into 4.12, gives via 4.6 the two equilibrium statements,

$$- \sigma^{\infty} \cos\beta \cos(\bar{\phi} + \phi) + \tau^{\infty} \sin(\beta + \bar{\phi} + \phi)$$

$$= \tau \sin(\beta - \bar{\phi} - \phi) + \sigma_L \cos(\beta - \bar{\phi} - \phi) \quad (4.15)$$

and $$\sigma^{\infty} \cos\beta \sin(\bar{\phi} + \phi) + \tau^{\infty} \cos(\beta + \bar{\phi} + \phi)$$

$$= \tau \cos(\beta - \bar{\phi} - \phi) + \sigma_T \sin(\beta - \bar{\phi} - \phi) \quad (4.16)$$

The longitudinal stress $\sigma_L$ along the fibre direction in the band is of limited interest (the fibres are inextensional), and we consider equation 4.15 no further. The stress components $\sigma_T$ and $\tau$ are of interest, and appear explicitly in our suggested constitutive laws for the band; we shall make extensive use of equation 4.16 in the calculation of the buckling response of the kinked band.

Note that the stress rates $\dot{\sigma}_L$, $\dot{\sigma}_T$ and $\dot{\tau}$ defined with respect to the rotating fibres are objective stress rates which are not equal to the Jaumann stress rates. Nevertheless, they appear to be the natural choice.

## 5. ELASTIC MICROBUCKLING

In this section we calculate the buckling load and the post buckling response for an elastic composite under remote compressive axial stress $\sigma^{\infty}$ and remote shear stress $\tau^{\infty}$. Material inside and outside of the kinked band has a transverse stiffness $E_T$ and a shear stiffness G, such that,

$$\tau^{\infty} = G\gamma^{\infty}, \quad \tau = G\gamma, \quad \sigma_T = E_T e_T \quad (5.1)$$

For simplicity, we assume remote proportional loading,

$$\tau^{\infty} = e\sigma^{\infty} \tag{5.2}$$

where the dimensionless parameter e is fixed, and neglect the presence of any imperfections, $\bar{\phi} = 0$. Budiansky (1983) has argued elsewhere that imperfections produce only small knock-down factors upon the buckling load, and can be neglected.

First, we calculate the buckling load. We differentiate the equilibrium equation 4.16 with respect to $\phi$ and make use of equations 4.8, 4.10, 5.1 and 5.2, to give,

$$f_1(\phi)\,\frac{d(\sigma^{\infty}/G)}{d\phi} = f_2(\phi) \tag{5.3}$$

where, $f_1(\phi) \equiv \cos\beta\,\sin\phi + e\,\frac{\sigma^{\infty}}{G}\,\sin\beta\,\cos^2\beta\,\sin\phi$

$+ e\,\cos(\beta+\phi) + e^2\,\frac{\sigma^{\infty}}{G}\,\cos^2\beta\,\sin(\beta+\phi) - e\,\cos\beta\,\cos\phi$

$- e\,\frac{\tau}{G}\cos^2\beta\,\sin(\beta-\phi) + e\,\frac{E_T}{G}\cos\beta\,\sin\phi\,\tan(\beta-\phi)$

$+ e\,\frac{\sigma_T}{G}\cos^2\beta\,\cos(\beta-\phi)$

$$f_2(\phi) \equiv \cos(\beta-\phi) + \frac{\tau}{G}\sin(\beta-\phi)$$

$$+ \frac{E_T}{G}\sin(\beta-\phi)\,\tan(\beta-\phi) - \frac{\sigma_T}{G}\cos(\beta-\phi)$$

$$- \frac{\sigma^{\infty}}{G}\cos\beta\,\cos\phi + e\,\frac{\sigma^{\infty}}{G}\,\sin(\beta+\phi) \tag{5.4}$$

In the limit $\phi \to 0, f_1(\phi) \to 0$. Hence $f_2(0) = 0$ by equation 5.3, and the buckling load $\sigma_c^{\infty}/G$ is

$$\frac{\sigma_c^{\infty}}{G} = \frac{1 + \frac{E_T}{G}\,\tan^2\beta_o}{1 - 2\,e\,\tan\beta_o} \tag{5.5}$$

In equation 5.5, $\beta_o$ is defined as the limit of $\beta$ as $\phi \to 0$, and not the inclination of the band boundary at $\sigma^{\infty} = \tau^{\infty} = 0$.

That is, $\beta_o$ is the initial inclination at buckling.

Surprisingly, we find from equation 5.5 that a negative value of remote shear stress $\tau^\infty = e\,\sigma^\infty$ reduces the buckling load. For a fixed $\tau^\infty/\sigma^\infty$ value there exists a critical initial inclination $\beta_c$ such that $\sigma_c^\infty/G$ is a minimum; this is demonstrated in Fig. 5a.

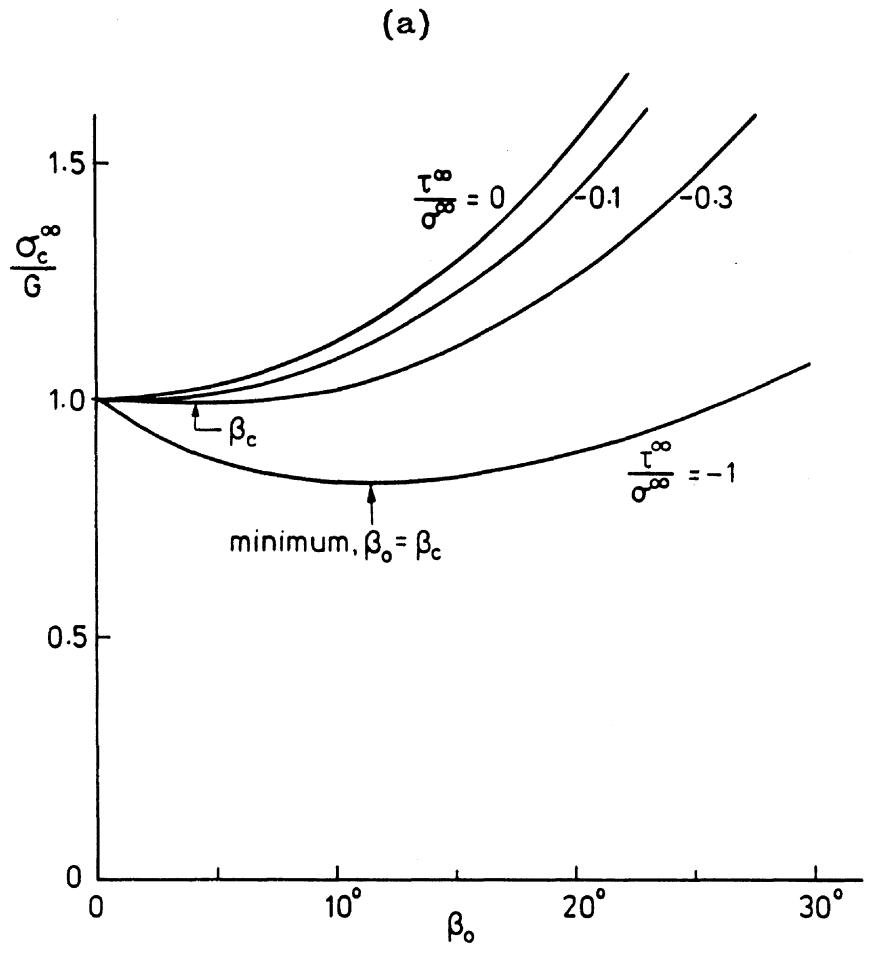


Fig.5(a): Effect of initial band inclination $\beta_o$ upon the elastic buckling stress $\sigma_c^\infty$, for the case $E_T/G = 4$.

An interaction diagram showing the buckling locus for $\beta_o = \beta_c$ is given in Fig. 5b. The collapse locus is sensitive to the value assumed for $E_T/G$, (Typically, $E_T/G \approx 4$). Equation 5.5 predicts $\beta_c = 0$ for the limit of vanishing remote shear stress. This is in disagreement with typical measurements of band angle for ceramic fibre polymer composites, where the observed angle is $\beta_o = 10° - 30°$. Budiansky (1983) argues via an elastic bending analysis that geometrical imperfections induce the onset of plastic yielding along an inclined domain at $\beta_o > 0$. Thus, in order to achieve $\beta_o > 0$ we must assume the presence of imperfections and assume the material is able to yield plastically.

(b)

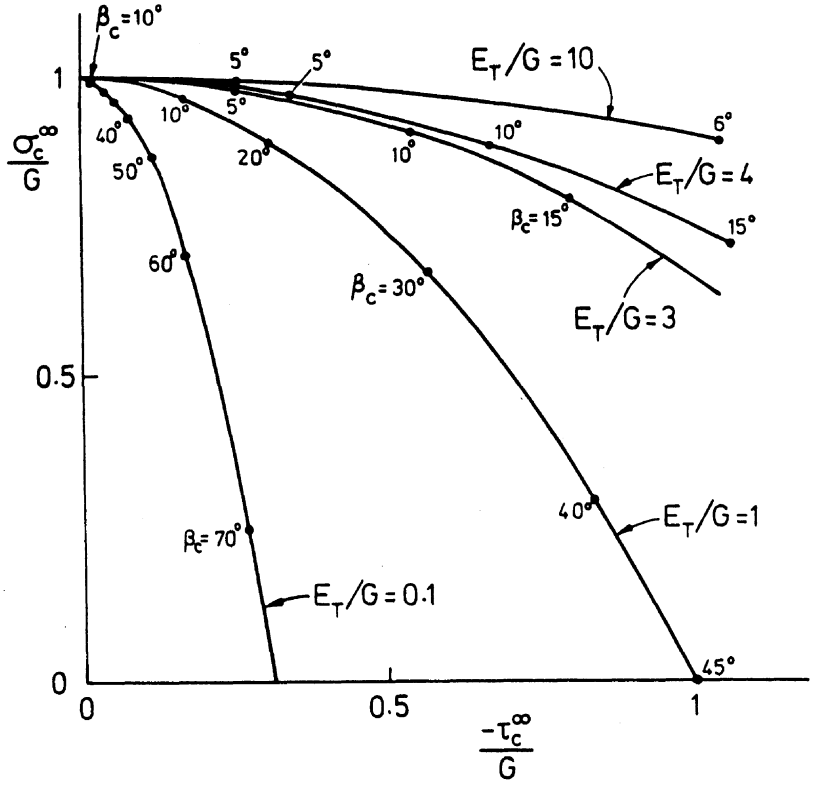


Fig.5(b): Interaction diagram for elastic microbuckling. Plot of buckling locus for weakest inclination $\beta_o = \beta_c$, for a range of $E_T/G$ values.

For most practical cases $E_T/G > 1$ and the presence of remote shear has only a small influence on the buckling load $\sigma^\infty_c/G$ as shown in Fig. 5b.

### 5.1 Elastic Post Buckling Response

The post buckling response is determined by integrating numerically a system of 4 linear 1st order differential equations:

$$\frac{d(\sigma^\infty/G)}{d\phi} = h_1\left(\frac{\sigma^\infty}{G}, \frac{\tau}{G}, \frac{\sigma_T}{G}, \beta, \phi\right)$$

$$\frac{d(\tau/G)}{d\phi} = h_2\left(\frac{\sigma^\infty}{G}, \frac{\tau}{G}, \frac{\sigma_T}{G}, \beta, \phi\right)$$

$$\frac{d(\sigma_T/G)}{d\phi} = h_3\left(\frac{\sigma^\infty}{G}, \frac{\tau}{G}, \frac{\sigma_T}{G}, \beta, \phi\right)$$

$$\frac{d\beta}{d\phi} = h_4\left(\frac{\sigma^\infty}{G}, \frac{\tau}{G}, \frac{\sigma_T}{G}, \beta, \phi\right) \qquad (5.6)$$

The function $h_1$ is given by $h_1 \equiv f_2/f_1$ from equations 5.3 and 5.4. Functions $h_2$, $h_3$ and $h_4$ follow naturally from equations 4.8, 4.10 and 5.1,

$$h_2 = 1 + e\frac{f_2}{f_1}\cos\phi\cos\beta\sec(\beta-\phi)$$

$$h_3 = \frac{E_T}{G}\tan(\beta-\phi) - e\frac{f_2}{f_1}\frac{E_T}{G}\sin\phi\cos\beta\sec(\beta-\phi)$$

$$\text{and } h_4 = -e\cos^2\beta\frac{f_2}{f_1} \qquad (5.7)$$

The system of equations 5.6 is integrated from $\phi = 0$ using a Runge-Kutta scheme. Since $f_1(\phi)$ and $f_2(\phi)$ are of order $\phi$ for $\phi$ small, care is required in evaluating $h_1 = f_2/f_1$ for small $\phi$.

Typical results are shown in Fig. 6. For $\beta_o = 0$ and all $\tau^\infty/\sigma^\infty$, the post buckling response is stable: $\sigma^\infty/G$ increases with increasing $\phi$. For $\beta_o > 0$,

a softening post bifurcation response is displayed. Now consider the effect of $\tau^\infty/\sigma^\infty$ upon the buckling response, as shown in Fig. 6. When $\tau^\infty/\sigma^\infty = 0$, the minimum buckling load $\sigma_c^\infty/G$ is achieved at $\beta_o = 0$. When $\tau^\infty/\sigma^\infty = -1$, $\sigma_c^\infty/G$ is a minimum at $\beta_o = 11.7°$; the post buckling response for this critical orientation is softening initially and hardening later. A snap-through response is predicted at large values of $|\tau^\infty/\sigma^\infty|$ and $\beta_o$, such as $\tau^\infty/\sigma^\infty = -1$, $\beta_o = 30°$.

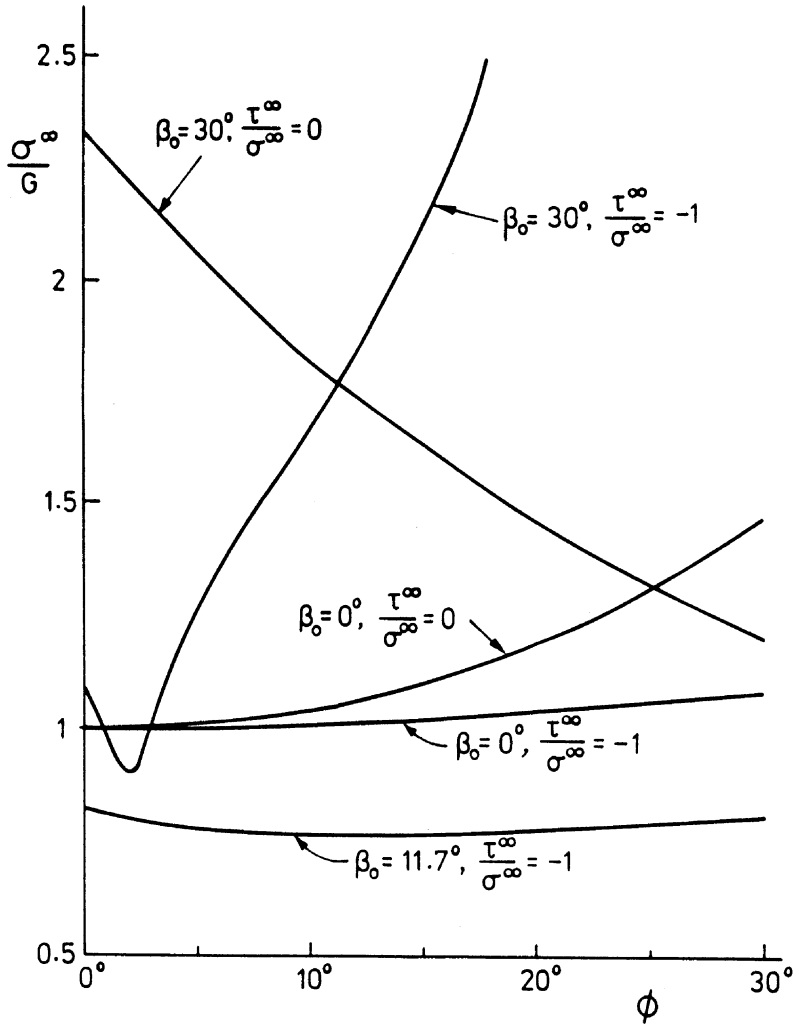


Fig.6: Elastic post buckling response, $E_T/G = 4$.

## 6. PLASTIC MICROBUCKLING

Polymer and metal matrix composites usually fail by plastic microbuckling. Budiansky (1983) has previously analysed plastic microbuckling by considering the response to remote axial stress $\sigma^\infty$ of a kink band made from rigid-perfectly plastic material. We begin by generalising this analysis for the case of a remote stress $\sigma^\infty$ with a remote shear stress $\tau^\infty$. Then, we consider microbuckling of an elastic-perfectly plastic solid under combined axial and shear stress. Plastic microbuckling in a strain hardening solid will be addressed in a future publication.

### 6.1 Rigid-Perfectly Plastic Solid

Consider the response of a rigid-perfectly plastic composite containing a kink band as shown in Fig. 4. The material is loaded remotely by an axial stress $\sigma^\infty$ and a shear stress $\tau^\infty$. In general, the kink band is inclined at an angle $\beta$, and fibres in the kink band suffer an initial misalignment $\bar{\phi}$.

During collapse, non-proportional plastic straining occurs in the kink band. Remote material remains rigid, thus $\beta$ is constant and we can drop the distinction between $\beta$ and $\beta_o$. Inclined kink bands induce transverse stresses at the initiation of kinking, so that a combined-stress plasticity law must be invoked. We use arbitrarily a quadratic yield condition,

$$\left(\frac{\tau}{k}\right)^2 + \left(\frac{\sigma_T}{\sigma_{Ty}}\right)^2 = 1 \qquad (6.1)$$

where k and $\sigma_{Ty}$ are the shear and tensile transverse yield stresses of the composite with respect to the fibre direction.

It appears reasonable to assume that an associated plastic flow rule applies. Then, by normality, $\dot{\gamma} = \frac{\tau}{k}\dot{\lambda}$

$$\dot{e}_T = \left(\frac{k}{\sigma_{Ty}}\right)^2 \frac{\sigma_T}{k}\dot{\lambda} \qquad (6.2)$$

where the non-dimensional parameter $\dot{\lambda}$ is positive for active plastic straining.

Combining equations 6.2 with equations 4.8 (recalling that $\dot{\gamma}^\infty = 0$ since remote material is rigid), gives,

$$\sigma_T = \tau \left(\frac{\sigma_{Ty}}{k}\right)^2 \tan(\beta - \bar{\phi} - \phi) \qquad (6.3)$$

and, via equation 6.1,

$$\tau = k\left(1 + \left(\frac{\sigma_{Ty}}{k}\right)^2 \tan^2(\beta - \bar{\phi} - \phi)\right)^{-\frac{1}{2}} \qquad (6.4)$$

We can now obtain an expression for the $\sigma^\infty$ versus $\phi$ collapse response, by substituting the equations 6.3 and 6.4 into 4.16,

$$\sigma^\infty = \frac{k\left(1+\left(\frac{\sigma_{Ty}}{k}\right)^2 \tan^2(\beta-\bar{\phi}-\phi)\right)^{\frac{1}{2}}\cos(\beta-\bar{\phi}-\phi) - \tau^\infty\cos(\beta+\bar{\phi}+\phi)}{\cos\beta\,\sin(\bar{\phi}+\phi)} \qquad (6.5)$$

For small $\bar{\phi}$ and $\phi$, this simplifies to,

$$\sigma^\infty \sim \frac{k^* - \tau^\infty}{\bar{\phi} + \phi} \qquad (6.6)$$

where $k^* \equiv k\left(1 + \left(\frac{\sigma_{Ty}}{k}\right)^2 \tan^2\beta\right)^{\frac{1}{2}}$ as given by equation

2.3. Equation 6.6 has been given previously by Batdorf and Ko (1987) in the limit $\beta = 0$. In the case of vanishing remote shear, equation 6.6 reduces to equation (2.2), given by Budiansky (1983).

For simplicity, we shall consider proportional remote loading with $\tau^\infty = e\sigma^\infty$. Equations 6.5 and 6.6 then reduce to,

$$\frac{\sigma^\infty \bar{\phi}}{k^*} = \left[\frac{1+(\frac{\sigma_{Ty}}{k})^2\tan^2(\beta-\bar{\phi}-\phi)}{1+(\frac{\sigma_{Ty}}{k})^2\tan^2\beta}\right]^{\frac{1}{2}} \frac{\cos(\beta-\bar{\phi}-\phi)\ \bar{\phi}}{\cos\beta\sin(\bar{\phi}+\phi)+e\cos(\beta+\bar{\phi}+\phi)} \tag{6.7}$$

and,

$$\frac{\sigma^\infty \bar{\phi}}{k^*} = (1 + \frac{e}{\bar{\phi}} + \frac{\phi}{\bar{\phi}})^{-1} \tag{6.8}$$

respectively.

**Results**

Equations 6.7 and 6.8 are compared in Fig. 7. We

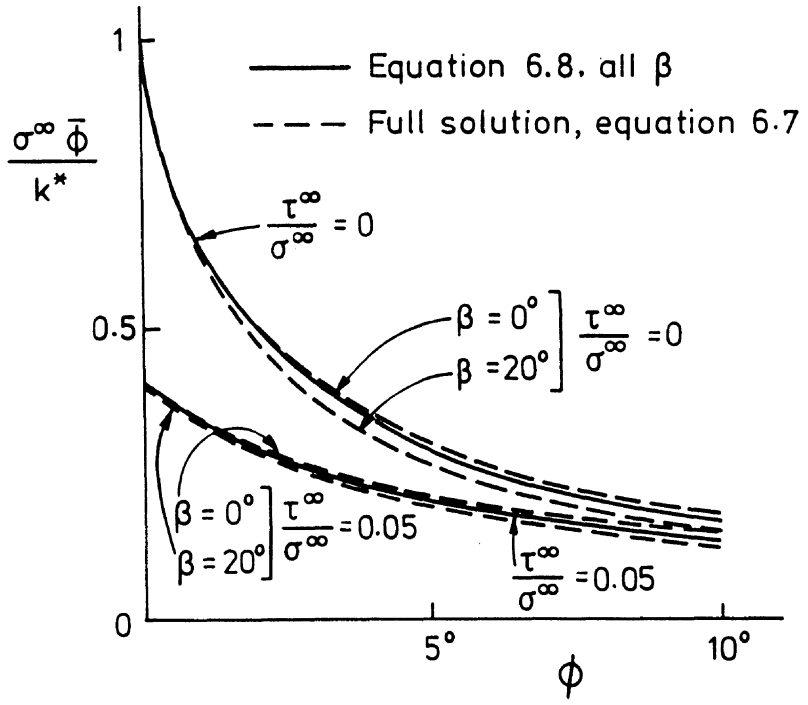


Fig.7: Accuracy of small $\phi$ approximation for microbuckling of a rigid-perfectly plastic solid. $\sigma_{Ty}/k = 2$, $\bar{\phi} = 2°$.

deduce that the small $(\bar{\phi} + \phi)$ approximation is adequate. Matrix failure or fibre-matrix debonding occurs at small values of $\phi$ (typically 3°) and the kink band then loses its load carrying capacity. Thus, equation 6.8 suffices over the range of validity of the analysis.

It is evident from equation 6.8 that the maximum value of remote stress $\sigma^{\infty}$ (at $\phi = 0$) is critically dependent upon the misalignment angle $\bar{\phi}$. As $\bar{\phi}$ tends to zero, $\sigma^{\infty}$ becomes unbounded; there is no finite bifurcation load for the perfect structure. The implication is that the materials manufacturer should arrange processing conditions to maximise fibre alignment, and thereby minimise $\bar{\phi}$.

We also deduce from equation 6.8 that a positive shear stress $\tau^{\infty}$ reduces the buckling stress $\sigma^{\infty}$. This contrasts with the case of elastic microbuckling where a negative value of $\tau^{\infty}$ reduces the bifurcation value of $\sigma^{\infty}$. To gain insight into this apparent paradox we consider next the buckling response of an elastic-perfectly plastic solid.

## 6.2 Elastic-perfectly Plastic Solid

We now examine the buckling response of an elastic-perfectly plastic composite, of geometry shown in Fig. 4. Consider the general case of the kink band inclined at an angle $\beta$, loaded remotely by $\sigma^{\infty}$ and $\tau^{\infty}$. The fibres in the band have an initial misalignment $\bar{\phi}$.

Typically, the response consists of two stages:

(a) An initial elastic response, followed by

(b) Matrix yielding and an elastic-plastic response.

We are interested in the early stages of deformation, and assume that $\phi$, the various strain measures and $\bar{\phi}$ are each small, such that equations 4.8 simplify to,

$$\gamma \sim \phi + \gamma^{\infty}, \qquad e_T \sim \phi \tan \beta \tag{6.9}$$

The shear strain in the remote material $\gamma^{\infty}$ remains less than the shear yield strain $\gamma_y$ (= 0.1%-1%) throughout the response. Thus $\beta \approx \beta_o$ by equation 4.11.

**(a) Initial Elastic Response**

The equilibrium equation 4.16, the constitutive law 5.1 and equation 6.9 may be combined to give the initial elastic response,

$$\sigma^{\infty} \sim \frac{(G + E_T \tan^2 \beta)}{(1 - 2\, e \tan \beta)} \frac{\phi}{\bar{\phi} + \phi} \tag{6.10}$$

Here, as elsewhere, we assume remote proportional loading with $\tau^{\infty} = e\, \sigma^{\infty}$.

The matrix yields when equation 6.1 is satisfied. At this instant $\phi$ attains the yield value $\phi_y$. Application of 5.1 and 6.9 gives,

$$\tau = G\gamma = G(\phi_y + e \frac{\sigma^{\infty}}{G})$$

$$\sigma_T = E_T e_T = E_T \phi_y \tan \beta \tag{6.11}$$

The value of $\sigma^{\infty}$ at which yield commences, $\sigma^{\infty} = \sigma^{\infty}_y$, is determined by substituting equation 6.10 and 6.11 into

the yield condition 6.1, and solving for $\sigma^\infty$ by the Newton-Raphson method. Predictions are compared in Fig. 8a with the buckling stresses $\sigma_c^\infty$, $\tau_c^\infty$ for a rigid-perfectly plastic solid,

$$\sigma_c^\infty = \frac{k^* - \tau_c^\infty}{\bar{\phi}} \qquad (6.12)$$

which is a restatement of equation 6.6 with $\phi = 0$.

It is clear from Fig. 8a that the collapse locus given by the rigid-perfectly plastic solid well

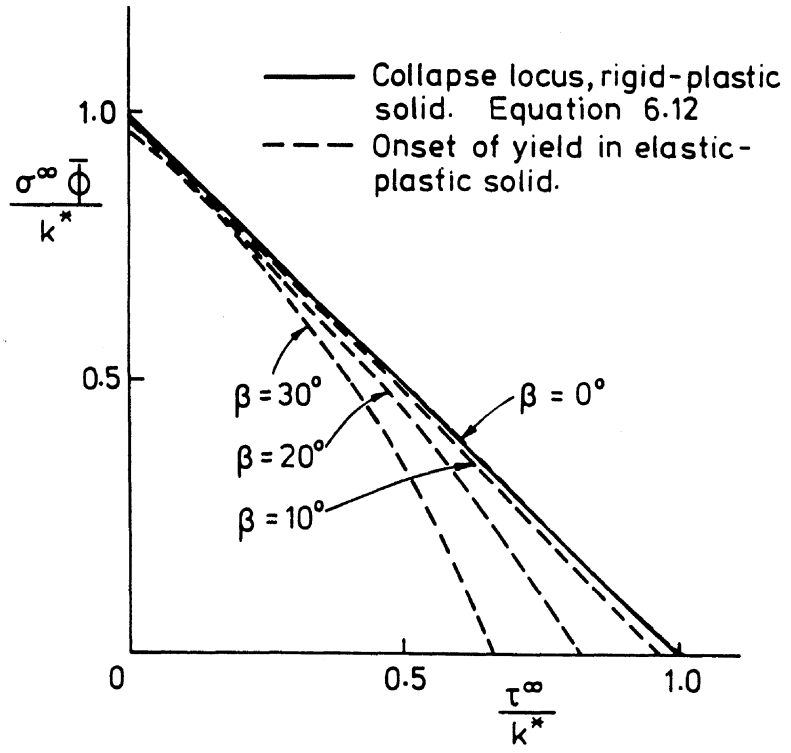


Fig.8(a): Comparison of collapse load $\sigma_c^\infty \bar{\phi}/k^*$ for rigid-perfectly plastic solid with onset of yield load $\sigma_y^\infty \bar{\phi}/k^*$ for elastic-perfectly plastic solid. $E_T/G = (\sigma_{Ty}/k)^2 = 4$, $\bar{\phi} = 2°$, $\gamma_y \equiv k/G = 0.001$.

approximates the onset of yield in the elastic-perfectly plastic solid. A positive shear stress $\tau^\infty$ decreases both the buckling stress $\sigma_c^\infty$ for the rigid-perfectly plastic solid, and the stress $\sigma_y^\infty$ at which the matrix yields for the elastic-perfectly plastic solid. In the limit of $e/\bar{\phi} \ll 1$ and $\phi/\bar{\phi} \ll 1$, $\sigma_y^\infty$ and $\sigma_c^\infty$ reduce to the same expression,

$$\sigma_y^\infty \sim \sigma_c^\infty \sim k^* \left(1 - \frac{e}{\bar{\phi}}\right) \qquad (6.13)$$

Consider the special case $\tau^\infty = 0$. Then equations 6.11 and 6.1 give,

$$\phi_y = \frac{k}{G}\left(1 + \left(\frac{k}{\sigma_{Ty}}\right)^2 \left(\frac{E_T}{G}\right)^2 \tan^2\beta\right)^{-\frac{1}{2}} \qquad (6.14)$$

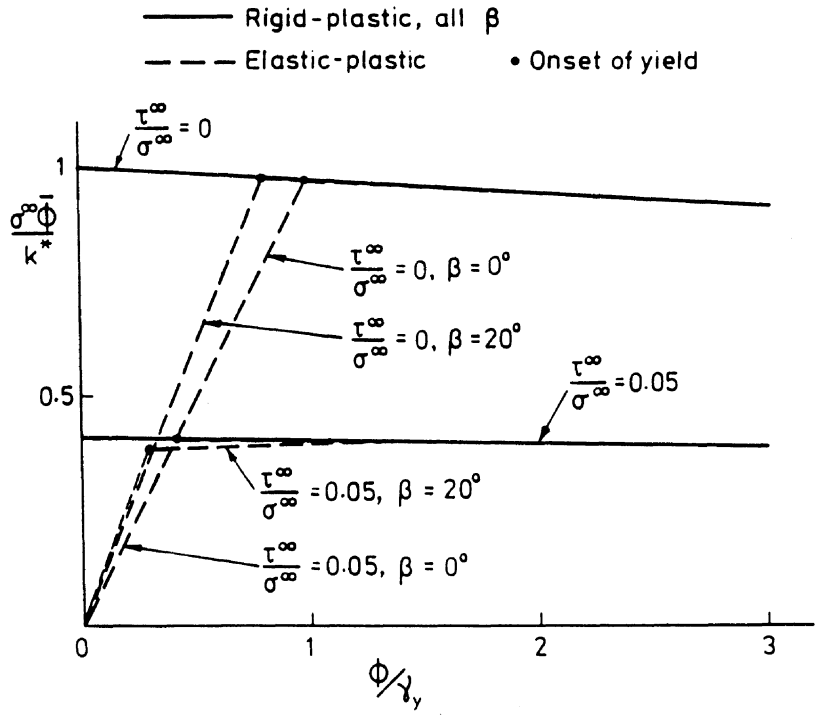


Fig.8(b): Comparison of collapse response for rigid-perfectly plastic solid with that for elastic-perfectly plastic solid. $E_T/G = (\sigma_{Ty}/k)^2 = 4$, $\bar{\phi} = 2°$, $\gamma = 0.001$.

If we assume for mathematical convenience $\frac{E_T}{G} = (\frac{\sigma_{Ty}}{k})^2$, then equations 6.10 and 6.14 reduce to,

$$\sigma_y^\infty = \frac{k^*}{\bar{\phi} + \phi_y} \tag{6.15}$$

where $k^* \equiv k\ (1 + (\frac{\sigma_{Ty}}{k})^2\ \tan^2\ \beta)^{\frac{1}{2}}$, as before. This value for $(\sigma_y^\infty,\ \phi_y)$ lies on the $\sigma^\infty$ versus $\phi$ response for the rigid-perfectly plastic solid given by equation 6.6.

**(b) Post Yield Response**

After matrix yield, the elastic-perfectly composite suffers both elastic and plastic straining in the kink band. The plastic strain rate is normal to the yield locus given by equation 6.1. A derivation of the relevant equations is given in Appendix A. Here, we describe only the results.

The pre and post yield response for the elastic-perfectly plastic solid is compared in Fig. 8b with the post buckling response for the rigid-perfectly plastic solid. We note that the matrix yields at $\phi/\gamma_y \lesssim 1$, where $\gamma_y = k/G$ is the shear yield strain of the matrix. The elastic-plastic response quickly approaches the rigid-perfectly plastic result, so that they are indistinguishable beyond $\phi/\gamma_y = 2$. We conclude that the rigid-perfectly plastic constitutive description is adequate for practical purposes.

In the limit of $\tau^\infty = 0$, with $\frac{E_T}{G} = (\frac{\sigma_{Ty}}{k})^2$, the post-yield elastic-perfectly plastic response coincides with the rigid-perfectly plastic response. In the

limit of $\beta = 0$, material in the kink band suffers simple shear with $\tau = k$, $\sigma_T = 0$. Again, the post yield elastic-perfectly plastic response coincides with the rigid-perfectly plastic response.

## 7. PROPAGATION OF A MICROBUCKLE BAND

In practice, fibre microbuckling initiates at a stress raiser such as an imperfection or a hole in a sheet. The microbuckle band propagates across the remaining section of the structure. Fleck and co-workers (Soutis and Fleck (1990), Soutis, Fleck and Smith (1990)) have analysed the early stages of microbuckle propagation by treating the microbuckle as a crack with a bridging zone at its tip. This approach is reasonable if the traction is negligible across the microbuckled band, at a distance far behind the tip of the advancing microbuckle.

Here, we calculate the stress $\sigma^{\infty}_{p}$ required to propagate a long microbuckle in steady state. In this limit, the rubble strength of the microbuckled material is not negligible. The geometry is shown in Fig. 9a. We assume remote proportional loading where $\tau^{\infty} = e\sigma^{\infty}$ and e is fixed. We shall use a simple energy argument to calculate $\sigma^{\infty}_{p}$, and make use of the remote stress versus remote displacement response of a microbuckled band of infinite length. Chater and Hutchinson (1984) used a similar method to calculate the pressure required to propagate bulges and buckles in elastic cylinders.

The predicted remote stress $\sigma^{\infty}$ versus $\phi$ response of the infinite band is shown in Fig. 9b. We

assume the infinite band displays the rigid-perfectly plastic characteristic, equation 6.6, for small $\phi$. When a critical fibre rotation $\phi_1$ is attained, the tensile transverse strain in the band $e_T$ equals the failure strain $e_{Tf}$ (typically $e_{Tf}$ = 1%) and the matrix fails, see Fig. 9b. The band strength vanishes with continued fibre rotation $\phi$ until $e_T$ reduces to zero at $\phi = \phi_2$. Thereafter we imagine the fibres in the band

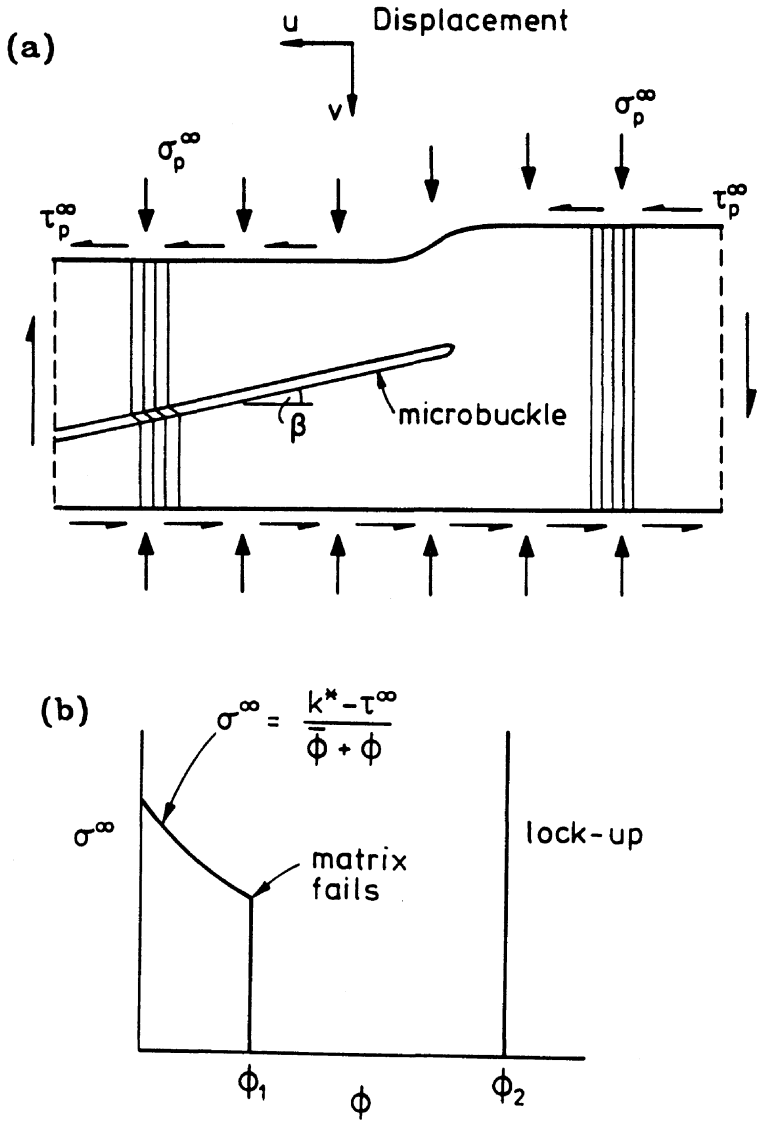


Fig.9: (a) Geometry of a propagating microbuckle. (b) Conjectured collapse response of a microbuckle.

contact each other and the band locks-up, with no further straining of the band. Lock-up is based on the idea that the composite resists compressive transverse straining in a highly stiff manner. The condition $e_T = 0$ corresponds to zero volumetric strain in the band since the fibres are considered to be inextensional. Chaplin (1977) and Evans and Adler (1978) also argue that fibre rotation stops when the volumetric strain in the band vanishes; they base their arguments on direct measurements of microbuckling.

Consider conservation of energy when the semi-infinite microbuckle shown in Fig. 9a undergoes a unit advance. For a deformation theory solid we get,

$$\sigma^{\infty}_{p}\, v_2 + \tau^{\infty}_{p}\, u_2 = \int_0^{v_1} \sigma^{\infty}\, dv + \int_0^{u_1} \tau^{\infty}\, du + G_c \sec\beta \quad (7.1)$$

where $\underset{\sim}{\sigma}_p$ is the fixed remote stress. Horizontal displacement u and vertical displacment v are defined in Fig. 9a. The first two terms on the right hand side of equation 7.1 refer to the work done by microbuckling when material is taken from a state $\phi = o$ to a state $\phi = \phi_2$, as shown in Fig. 9b. The last term on the right hand side of equation 7.1 represents the dissipation due to delamination and damage in off-axis plies.

Equation 7.1 provides a **necessary** condition for microbuckling: a detailed collapse mechanism at the tip of the advancing microbuckle would provide the **sufficient** condition.

We next calculate $\sigma^{\infty}_{p}$ from equation 7.1. The matrix fails when $e_T = e_{Tf}$ at a fibre rotation $\phi_1$,

$$\phi_1 = \frac{e_{Tf}}{\tan\beta - \bar{\phi}\sec^2\beta} \quad (7.2)$$

Lock-up occurs when $e_T$ equals zero. This is achieved at a fibre rotation $\phi_2$, where by 4.9,

$$\phi_2 = 2(\beta - \bar{\phi}) \tag{7.3}$$

By kinematics, the remote displacements u and v, which form the work conjugates of $\tau_p^\infty$ and $\sigma_p^\infty$ respectively, are,

$$\frac{u}{w} = \sin(\bar{\phi} + \phi) - \sin\bar{\phi}$$
$$\frac{v}{w} = \cos\bar{\phi} - \cos(\bar{\phi} + \phi) \tag{7.4}$$

When $\phi$ is small, these reduce to,

$$\frac{u}{w} = \phi$$
$$\frac{v}{w} = \tfrac{1}{2}\phi^2 + \bar{\phi}\phi \tag{7.5}$$

Equation 7.1 can be evaluated using equations 6.6, 7.2-7.5 and the assumption of proportional remote loading $\tau^\infty = e\,\sigma^\infty$ to give,

$$\frac{\sigma_p^\infty}{k} = [(1-\cos2\beta - \bar{\phi}\sin2\beta) + e(\sin2\beta - \bar{\phi}(1 + \cos2\beta))]^{-1}$$
$$\times [\phi_1 (1 + (\frac{\sigma_{Ty}}{k})^2 \tan^2\beta)^{\frac{1}{2}} + \frac{G_c}{kw}\sec\beta] \tag{7.6}$$

where $\phi_1$ is specified by equation 7.2.

The buckle propagation stress $\sigma_p^\infty$ is plotted against band inclination $\beta$ in Fig. 10, by evaluating equation 7.6. We note that $\sigma_p^\infty$ increases with increasing $G_c$ and decreasing $\tau^\infty$, as expected. A critical angle of $\beta$ exists for which $\sigma_p^\infty$ is a minimum, for any specified material parameters and loading ratio e. Disappointingly, the predicted values of $\beta$ are in the range 45° - 75° which are larger than the values 10° - 30° typically measured. This suggests that the angle $\beta$ may be set and locked-in at the initiation of kink

propagation, by deformation patterns induced elastically via initial misalignments, as proposed by Budiansky (1983).

The kink band analysis does not provide us with the value of the kink width w. Budiansky (1983) has predicted w with reasonable success using an elastic bending analysis. He finds for perfectly brittle fibres (tensile failure strain = 0),

$$\frac{w}{d} = \frac{\pi}{4}\left(\frac{2\,k^*}{v_f E}\right)^{-\frac{1}{3}} \qquad (7.7)$$

where d is the fibre diameter. This expression predicts correctly w/d ~ 10 for material properties typical of carbon fibre epoxy composites.

### 7.1 Case Study

Soutis and Fleck (1990) have examined recently the

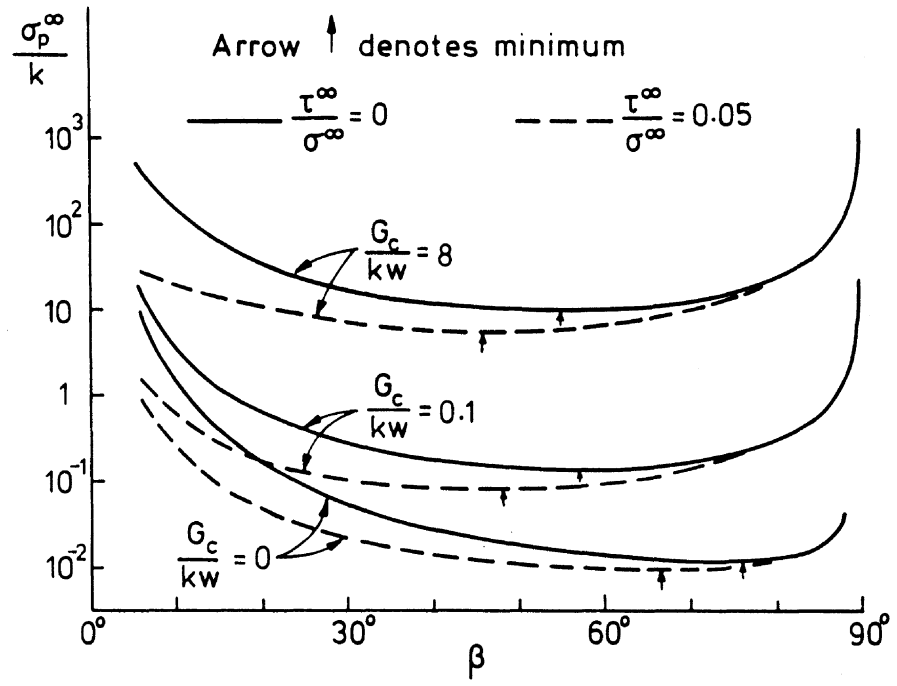


Fig.10: Effect of band angle $\beta$ upon propagation stress $\sigma_p^\infty/k$. $\sigma_{Ty}/k = 2$, $\bar{\phi} = 2°$, $e_{Tf} = 0.01$.

compressive failure of a unidirectional and $[\pm 45°/0_2)_3]_s$ multidirectional carbon fibre epoxy composite. They measured the following material properties for the unidirectional material under remote axial loading: $\beta = 20°$, $k = 60$ MPa, $E_T/G = (\sigma_{Ty}/k)^2 = 4$, $\sigma_c = 1600$ MPa. Equation 6.6 predicts $\bar{\phi} = 2.6°$ which is consistent with the level of fibre misalignment observed. The fibre rotation after microbuckling $\phi_2$ was found to satisfy equation 7.3, supporting the concept of lock-up. Soutis and Fleck were unable to measure the buckle propagation stress $\sigma_p^\infty$ since unstable buckle propagation occurred once the microbuckle was initiated. This is consistent with the predicted value $\sigma_p^\infty = 13$ MPa from equation 7.6 which is much less than the measured buckling strength $\sigma_c = 1600$ MPa.

Soutis and Fleck (1990) have also measured the toughness $G_c$ associated with splitting and delamination in the $[(\pm 45/0_2)_3]_s$ laminate. They measured $G_c = 30$ kJ/m$^2$ from the compressive fracture load of specimens containing central slits transverse to the loading direction. This value for $G_c$ together with an observed value for $w = 60\mu$m, gives $G_c/kw = 8.3$, and $\sigma_p^\infty = 2900$ MPa via equation 7.6. This predicted value for $\sigma_p^\infty$ is too high, as the multi-directional laminate was observed to fail unstably at a stress $\sigma_c = 810$ MPa. We conclude that more detailed modelling of damage development in the off-axis plies is required. This is not surprising, since the measured toughness $G_c$ associated with delamination and splitting is more than two orders of magnitude greater than the dissipation

due to microbuckling per unit area advance of the microbuckle.

## 8. CONCLUDING REMARKS

The elastic and plastic kinking analyses of microbuckling is able to account for some but not all of the experimental observations. Fibre bending must be treated explicitly in order to predict the width w of the microbuckle band and the band inclination $\beta$.

There remains a paucity of experimental evidence on the underlaying features of microbuckling. The authors are unaware of any systematic studies which examine the influences of fibre misalignment upon microbuckling strength. It is difficult to distinguish experimentally between elastic and plastic microbuckling of polymer matrix composites, as matrix yield stress usually scales linearly with matrix stiffness. Data on the shape of the yield locus for composites remain scant. It seems that few systematic experimental studies have been conducted of the elastic microbuckling of fibre composites with elastomeric matrices.

The buckle propagation analysis suggests that only a small compressive stress is required in order to propagate an existing microbuckle. No measurements of the microbuckle propagation stress were found from the literature.

## ACKNOWLEDGEMENTS

This work was supported in part by DARPA University Research Initiative (Subagreement P.O. NO.

VB38639-0 with the University of California, Santa Barbara, ONR Prime Contract 00014-86-K-0753), and by the Division of Applied Sciences, Harvard University. The authors are also grateful for funding from the Procurement of Executive of the Ministry of Defence, under a joint SERC/MOD contract.

## APPENDIX A: DERIVATION OF POST-YIELD ELASTIC-PERFECTLY PLASTIC RESPONSE

The post-yield elastic-perfectly plastic response is given in rate form as follows. We shall use the superscripts e and p to denote elastic and plastic, respectively. The strain rate in the kink band is,

$$\dot{\gamma} = \dot{\gamma}^e + \dot{\gamma}^p, \quad \dot{e}_T = \dot{e}_T^e + \dot{e}_T^p \tag{A1}$$

where,

$$\dot{\gamma}^e = \frac{\dot{\tau}}{G}, \quad \dot{e}_T^e = \frac{\dot{\sigma}_T}{E_T} \tag{A2}$$

in accordance with equations 5.1, and

$$\dot{\gamma}^p = \frac{\tau}{k}\dot{\lambda}, \qquad \dot{e}_T^p = \left(\frac{k}{\sigma_{Ty}}\right)^2 \frac{\sigma_T}{k}\dot{\lambda} \tag{A3}$$

by equations 6.2; $\dot{\lambda}$ is a positive number for active plastic straining. Assume proportional remote loading with $\tau^\infty = e\sigma^\infty$. We combine equations A1-A3, with the yield condition 6.1 and the kinematic relations 4.8, to obtain $\dot{\lambda}$ and the stress rates in the kink band $\dot{\tau}$ and $\dot{\sigma}_T$,

$$\begin{bmatrix} \dot{\tau}/G \\ \dot{\lambda} \end{bmatrix} = \frac{1}{A}\begin{bmatrix} A_{11} & A_{12} \\ A_{21} & A_{22} \end{bmatrix}\begin{bmatrix} \dot{\phi} \\ \dot{\sigma}^\infty/G \end{bmatrix}$$

$$A \equiv \frac{\sigma_T}{k}\left(\frac{k}{\sigma_{Ty}}\right)^2 + \frac{\tau}{k}\frac{\tau}{\sigma_T}\left(\frac{\sigma_{Ty}}{k}\right)^2 \frac{G}{E_T}$$

$$A_{11} = \frac{\sigma_T}{k}\left(\frac{k}{\sigma_{Ty}}\right)^2 - \frac{\tau}{k}\tan\left(\beta - \bar{\phi} - \phi\right)$$

$$A_{12} = \left[\frac{\sigma_T}{k}\left(\frac{k}{\sigma_{Ty}}\right)^2 \cos(\bar{\phi}+\phi) + \frac{\tau}{k}\sin(\bar{\phi}+\phi)\right] e \cos\beta \sec(\beta-\bar{\phi}-\phi)$$

$$A_{21} = \frac{\tau}{\sigma_T}\left(\frac{\sigma_{Ty}}{k}\right)^2 \frac{G}{E_T} + \tan\left(\beta-\bar{\phi}-\phi\right)$$

$$A_{22} = \left[\frac{\tau}{\sigma_T}\left(\frac{\sigma_{Ty}}{k}\right)^2 \frac{G}{E_T}\cos(\bar{\phi}+\phi) - \sin(\bar{\phi}+\phi)\right] e \cos\beta \sec(\beta-\bar{\phi}-\phi)$$

$$\dot{\sigma}_T = -\frac{\tau}{\sigma_T}\left(\frac{\sigma_{Ty}}{k}\right)^2 \dot{\tau} \qquad \text{(A4)}$$

Equations A4 simplify in an obvious manner when we assume small $(\bar{\phi}+\phi)$, and $E_T/G \equiv (\sigma_{Ty}/k)^2$. To proceed, we differentiate the equilibrium equation 4.16 with respect to time, and substitute for $\dot{\tau}$, $\dot{\sigma}_T$ using A4, and for $\dot{\beta}$ using 4.10. This results in a 1st order differential equation for $d(\sigma^\infty/G)/d\phi$ of the type given in 5.6, but with a new expression for $h_1$. Similarly, we obtain 1st order differential equations for $d(\tau/G)/d\phi$, $d(\sigma_T/G)/d\phi$ and for $d\beta/d\phi$. The resulting system of 1st order differential equations, analogous to equations 5.6, is integrated numerically using a Runge-Kutta routine. The starting values are given by the onset of yield condition described in part (a) of section 6.2. Results are shown in Fig. 8b.

**REFERENCES**

Argon, A.s. (1972). "Fracture of composites", Treatise of Materials Science and Technology, Vol. 1, Academic Press, New York.

Barker, A.J. and Balasundaram, V. (1987). "Compression testing of carbon fibre-reinforced plastic exposed to humid environments", Composites, 18(3), pp. 217-226.

Batdorf, S.G. and Ko, R.W.C. (1987). "Stress-strain behaviour and failure of uniaxial composites in combined compression and shear, Parts I and II, "Internal report, School of Engineering and Applied Science, University of California, Los Angeles, CA 90024.

Budiansky, B. (1983). "Micromechanics", Computers and Structures, 16(1), pp. 3-12.

Chaplin, C.R. (1977). "Compressive fracture in unidirectional glass-reinforced plastics", J.Mat.Sci., 12, pp. 347-352.

Chater, E. and Hutchinson, J.W. (1984). "On the propagation of bulges and buckles", J.Appl.Mech., 51, pp. 269-277.

Curtis, P.T. and Bishop, S.M. (1984). "An assessment of the potential of woven carbon fibre reinforced plastics for high temperature applications, Composites, 15(4), pp. 259-265.

Dow, N.F. and Gruntfest, I.J. (1960). "Determination of most-needed, potentially possible improvements in materials for ballistic and space vehicles". General Electric, Air Force Contract AF04(647)-269.

Evans, A.G. and Adler, W.F. (1978). "Kinking as a mode of structural degradation in carbon fiber composites", Acta Metallurgica, 26, pp. 725-738.

Ewins, P.D. and Ham, A.C. (1973). "The nature of compressive failure in unidirectional carbon fibre reinforced plastic", RAE Technical Report 73057.

Ewins, P.D. and Potter, R.T. (1980). "Some observations on the nature of fibre reinforced plastics and the implications for structural design", Phil.Trans.R.Soc.Lond., A294, pp. 507-517.

Greszczuk, L.B. (1972). "Failure mechanisms of composites subjected to compressive loading", AFML-TR-72107, U.S. Air Force.

Greszczuk, L.B. (1975). "Microbuckling failure of circular fibre-reinforced composites", AIAA Journal, 13 (10), pp. 1311-1318.

Jelf, M. (1990), unpublished research, Cambridge University Engineering Dept., England.

Lager, J.B. and June, R.R. (1969). "Compressive strength of boron/epoxy composites", J.Composite Material, 3(1), pp. 48-56.

Moncunill de Ferran E. and Harris, B. (1970). "Compression of polyester resin reinforced with steel wires". J.Comp.Mater. 4, p.62.

Piggott, M.R. and Harris, B. (1980). "Compression strength of carbon, glass and Kevlar-49 fibre reinforced polyester resins", J.Mat.Sci., 15, pp. 2523-2538.

Piggott, M.R. (1981). "A theoretical framework for the compressive properties of aligned fibre composites", J.Mat.Sci., 16, pp. 2837-2845.

Rosen, B.W. (1965). "Mechanics of composite strengthening", Fibre Composite materials, Am.Soc.Metals Seminar, Chapter 3.

Rhodes, M.D., Mikulas, M.M. and McGowan, P.E. (1984). "Effects of orthotrophy and width on the compression strength of graphite-epoxy panels with holes", AIAA Journal, 22(9), pp. 1283-1292.

Soutis, C. (1989). "Compressive failure of notched carbon fibre-epoxy panels", Ph.D. Thesis, Cambridge University Engineering Department, England.

Soutis, C. and Fleck, N.A. (1990). "Static compression failure of carbon fibre T800/924C composite plate with a single hole", to appear in June issue of J.Composite Materials.

Soutis, C., Fleck, N.A. and Smith, P.A. (1990). "Failure prediction technique for compression loaded carbon fibre-epoxy laminate with open holes", submitted to J.Composite Materials.

Starnes, J.H. and Williams, J.G. (1982). "Failure characteristics of graphite/epoxy structural components in compression", Mechanics of composites materials-recent advances, pp. 283-306, eds. Z. Hashin and C.T. Herakovich, Pergamon Press.

Steif, P. (1988). "A simple model for the compressive failure of weakly bonded, fiber-reinforced composites", J.Composite Materials, 22, pp.818-828.

U.S. Polymeric (1990). Data sheets on properties of carbon fibre epoxy composites, 700E Dyer Rd., Santa Ana, CA, 92707, USA.